

Experimental study on upward bubble velocity and pierce length distributions in a water model of copper converter

Bin Du^{1,2}, Jiayun Zhang¹, Tuping Zhou¹, and Qifeng Shu¹

1) Metallurgical Engineering School, University of Science and Technology Beijing, Beijing 100083, China

2) Legend Co. Ltd., Beijing 100085, China

(Received 2003-01-25)

Abstract: The upward bubble velocity and the pierce length distributions in a sectional water model of the copper converter in Guixi Smelter in Jiangxi, China, were measured using a two-contact electro-resistivity probe. In the case of using a single tuyere, the bubble velocity distribution along longitudinal direction was similar to that derived from Gaussian function. Beyond the center of the longitudinal range, the bubble pierce length exhibited a sudden increase. The upward bubble velocity at a specified location could go up to meters per second. Its probability at a fixed location obeys a lognormal function; the bubble pierce length there varies below a few centimeters. In the case of using multi-tuyeres, the upward bubble velocity was roughly uniform right above the tuyeres and showed a slow decrease beyond this region. The bubble pierce length within both of these two regions was roughly uniform. Its average value in the former region, however, was found to be somewhat lower than that in the later.

Key words: upward bubble velocity; bubble pierce length; distribution; copper converter

[This work was financially supported by the National Natural Science Foundation of China (No.59874005).]

1 Introduction

The void fraction, bubble size and velocity distribution characteristics in gas stirred metallurgical reactors are very important for understanding the process mechanism, even the evaluation of rate phenomena involved. The distribution studies of bubble size and velocity in water models stirred by bottom gas-injection can frequently be found in references [1-6]. A few others were carried out in a liquid metal bath [4-6] by using a magnetic probe.

Regarding the cases in the reactors with a horizontal gas injection, only a few reports for void fraction distributions can be found. These involve the studies by Oryall and Brimacombe [7] and by the present research group [8]. The former work was carried out in a more fundamental manner using a rectangular water container with a single nozzle. While the experiments in the later was performed in a sectional water model of a copper converter geometrically similar to that in Guixi Smelter, Jiangxi, China. The ratio of the model diameter to that of the prototype was 1:6.5. However, as a sectional model, the length of the model was much shorter, only 0.192 m, containing only five tuyeres. Two series of experiments, air-blowing

through a single tuyere as well as multi-tuyere, were carried out, so that effects of the interaction between the adjacent gas-liquid streams (plumes) through adjacent tuyeres in a copper converter bath could be examined.

As a continuation and extension of the previous study, the bubble size and velocity distributions in the present work have been investigated using the same water model and the same operating parameters. The results of the present study together with that attained before could provide a more complete description regarding the characteristics of the two-phase zone in a copper converter. This would be helpful for improving our understanding of the kinetic aspect during the copper converter operation.

2 Experimental

2.1 Experimental techniques

The technique of the two contact electroresistivity probe used in this work can refer to references [2, 3, 9]. The length for the bubble to be pierced between the lower and upper contacts of the probe is defined as the bubble pierce length. Based on statistics, it has been obtained that the average bubble diameter \bar{d}

measured at a specified location is proportional to the average pierce length, \bar{L}_b , as follows [9]:

$$\bar{d} = 3 \bar{L}_b \quad (1)$$

and the average velocity \bar{U}_b is defined as

$$\bar{U}_b = \sum_{i=1}^N U_b(i) / N \quad (2)$$

where $U_b(i)$ denotes the bubble velocity at the i th sampling, N is the total number of samples taken at a specified location. The two contacts of the probe are fixed in the way that they are right in the same vertical line. This implies only the upward-vertical component of the velocity can be measured, the term of 'bubble velocity' means the upward bubble velocity in this paper.

A computer program using QBasic and assemble language hybrid coding technique was applied to meet the higher data-acquisition demand. The computer data-acquisition system can count, record and store the contacting time difference for a bubble from the lower contact to the upper, and to convert it into the bubble velocity and pierce length data.

2.2 The experimental apparatus and procedure

The figure for experimental assembly for the measurements can be found in reference [8]. It consists of a converter model, an electroresistivity probe as well as the attached computer data-acquisition device. The dimensions of the model involve the water height level of 0.238 m and the model length of 0.192 m containing only 5 tuyeres. The inner diameter for all the tuyeres is 3 mm.

The airflow rate (S.T.P.) through each tuyere was 1.74 m³/h, the same as that for the void fraction measurement [8], so the equality of the modified Froude number Fr' and the dynamic similarity between the model and the prototype could be fulfilled. This means that the present study only emphasizes the distribution features of the bubble size and velocity, but not their absolute values.

As illustrated in **figure 1**, tuyeres 1, 2, 4, 5 were used for gas blowing by multi-tuyere. Tuyere 3 in the middle between tuyeres 2 and 4 was used for the gas blowing by single-tuyere type. This figure also gives the coordinate system setup for the measurements. The center of the orifice of tuyere 3 was set as the origin for the coordinate system. Section XOY , XOZ and YOZ are the main sections across origin. XY , XZ and YZ are parallel to those sections, respectively.

In order to ensure reasonable accuracy and precision, one thousand data were repeatedly taken during

the data acquisition at a specified point. The arithmetic means of the acquired data was taken as the time average values for the bubble velocity and the pierce length at the point being measured.

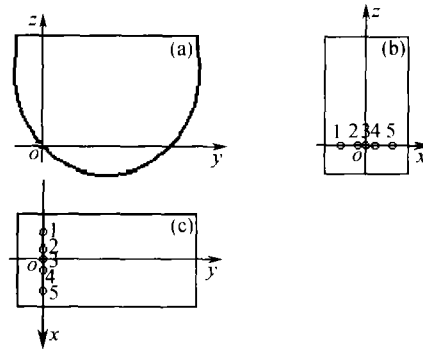


Figure 3 Schematic diagram of converter model, (a) Section YOZ ; (b) Section XOZ ; (c) Section XOY ; Numbers 1-5 mean tuyeres 1-5.

3 Results

3.1 Gas-blowing through a single tuyere

(1) In section XZ at $y = 35$ mm.

The distribution for either the bubble velocity or the pierce length can be revealed in a few characteristic sections. **Figures 2** and **3** illustrate the distributions of the measured bubble velocity and pierce length in the lower region of the vertical section XZ at $y=35$ mm, respectively. It is seen that both the bubble velocity and the pierce length show a similar distribution to Gaussian function, a maximum value occurs at $x=0$ for the every given height of the water level. It is noticed that $x=0$ corresponds to the X coordinate of the center of Tuyere 3. While the bubble velocity becomes uniform as depicted in **figure 4**. This may reflect that at higher levels in this section the horizontal velocity component has nearly diminished and all the forces exerting on the bubbles approach to be in balance. However, as indicated in **figure 5**, the pierce length in this region shows a complex distribution. It can be seen that the pierce length reduces with $|x|$ from a maximum at $x=0$ of each height level to $|x|=20$ mm. This bubble size reducing may be caused by the diverging of the gas-liquid stream. While beyond $|x|=20$ mm, the recirculating flow affected by the two vertical sidewalls may impinge the main stream, therefore, resulting a bubble coalescence.

(2) In section XOZ .

Section XOZ is an important plane in characterizing the bubble velocity and the pierce length distributions. **Figure 6** indicates the bubble velocity distribution in section XOZ . It can be seen that the main features either for the lower or the upper region are respectively the same as those in the lower or the upper part

of section XZ at $y=35$ mm. Comparing the bubble pierce length distribution in the lower and the upper zones of section XOZ shown in figure 7 respectively with those depicted in figures 3 and 5 could draw a similar conclusion. In figures 6 and 7, there is no data shown when $|x| > 12$ mm at $z=20$ mm, which was due to the instable data output in the measurement. It can also be noticed that the measured data are strongly non-linear with the water height level from 20 to 40 mm. The very different impingement effects of the surface flow along the vertical level might cause the non-linearity.

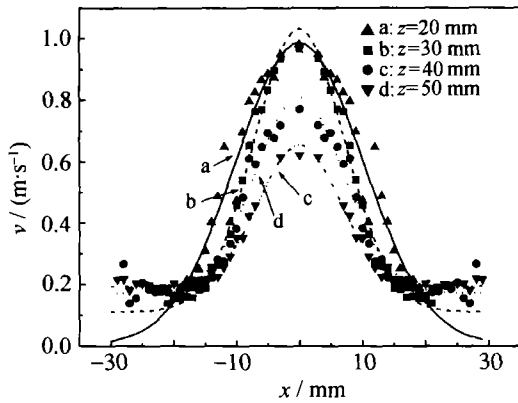


Figure 2 The bubble velocity distribution in the lower region of Section XZ at $y=35$ mm (using a single tuyere).

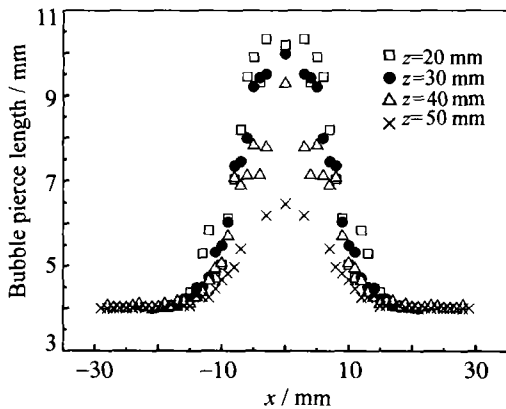


Figure 3 The bubble pierce length distribution in the lower region of Section XZ at $y=35$ mm (using a single tuyere).

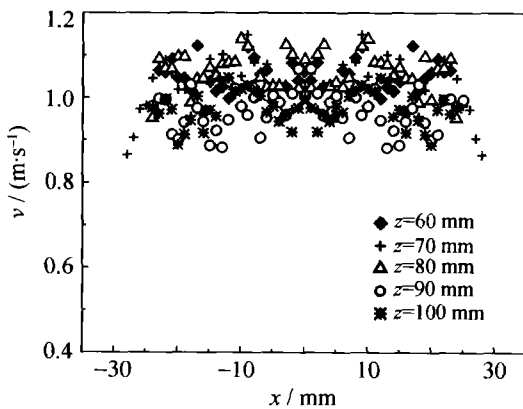


Figure 4 The bubble velocity distribution in the upper region of Section XZ at $y=35$ mm (using a single tuyere).

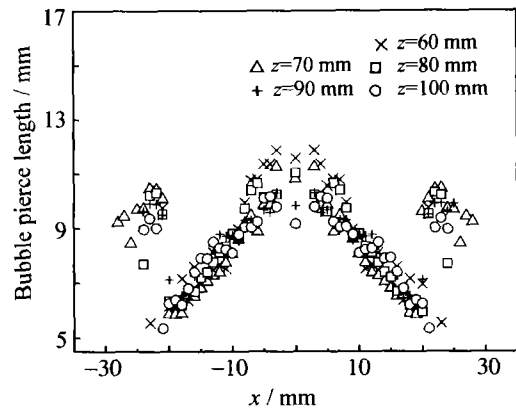


Figure 5 The bubble pierce length distribution in the upper region of Section XZ at $y=35$ mm (using a single tuyere).

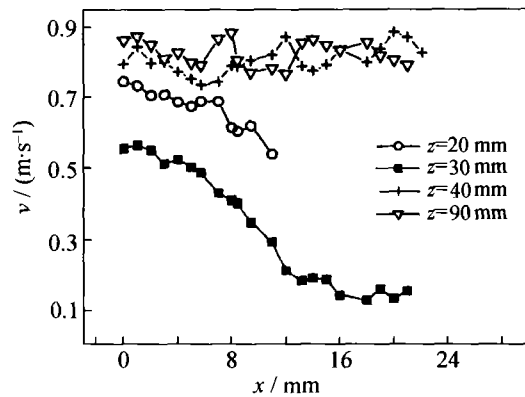


Figure 6 The bubble velocity distribution in Section XOZ (using a single tuyere).

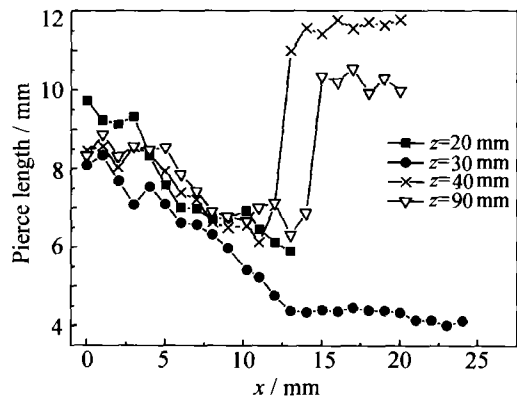


Figure 7 The bubble pierce length distribution in Section XOZ at $y=0$ mm (using a single tuyere).

(3) Distribution of the probability of the bubble velocity.

It has been noticed that the bubble velocity measured at a fixed point is varied in a wide range [6]. In the present study, the resultant probability distribution for the bubble velocity at a specified point can well fit to lognormal distribution given by equation (3).

$$\rho_v = \rho_{v_{max}} \exp \left\{ - \frac{[\ln(v_{max}) - \ln(v)]^2}{2[\ln(v_s)]^2} \right\} \quad (3)$$

where ρ_v stands for the distribution function of probability for the bubble velocity at a specified point, and

$\rho_{v, \max}$ is the maximum of ρ_v , v denotes the bubble velocity; v_{\max} is the maximum bubble velocity and v_e the error of the velocity measurement.

Figure 8 is a typical example obtained at a location where $x=0, y=35 \text{ mm}, z=30 \text{ mm}$. As shown in this figure, ρ_v is very small if the bubble velocity is less than 0.2 m/s. Above this value, ρ_v goes up abruptly and reaches a maximum at $v=0.7 \text{ m/s}$, then gradually reduces to a very low value where the bubble velocity approaches about 3 m/s. It is known from figure 2 that the average velocity at this location is about 0.9 m/s. Figure 9 indicates that $\rho_{v, \max}$ increases with x . Meanwhile the location where the maximum velocity occurs is gradually moving towards to $x=0$.

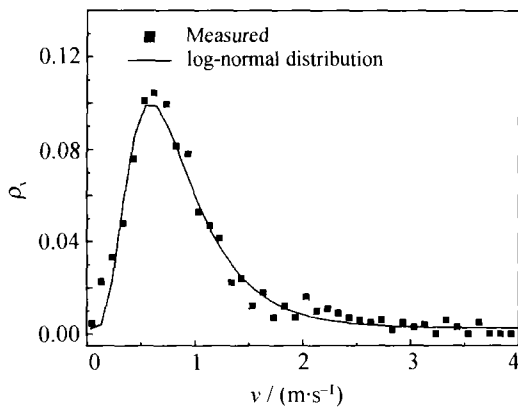


Figure 8 Comparison of measured probability distribution of bubble velocity at $x=0, y=35, z=30 \text{ mm}$ with log-normal distribution function (using a single tuyere).

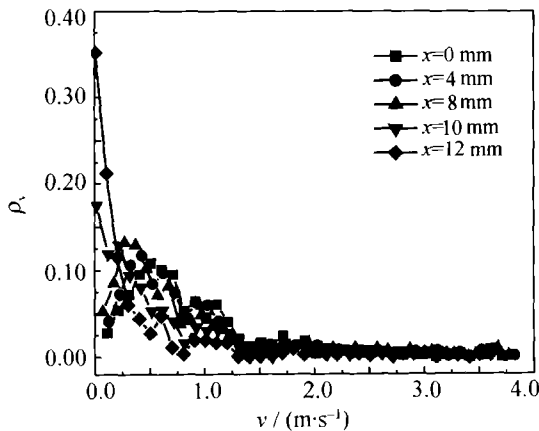


Figure 9 Distributions of probability of bubble velocity at different x locations where $y=35 \text{ mm}, z=20 \text{ mm}$ (using a single tuyere)

(4) Distribution of the probability of the bubble pierce length value.

Figure 10 gives probability distributions of bubble pierce length at several height levels where $x=0 \text{ mm}, y=35 \text{ mm}$. It is seen that for all the height levels, the bubble pierce length varies mainly within the same narrow range from 2 to 13 mm though the corre-

sponding maximum probability decreases with the increasing height level.

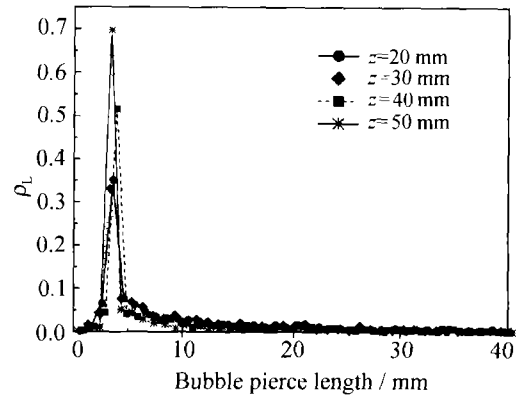


Figure 10 Distributions of probability of bubble pierce length (ρ_L) at different height levels where $x=0, y=35 \text{ mm}$ (using a single tuyere).

3.2 The Gas flow through multi-tuyere

(1) In section XZ at $y=35 \text{ mm}$.

In the copper converter operation, air is blown into the bath through closely and horizontally fixed 40-60 tuyeres along the longitudinal direction. In order to clarify the effect of the interactions between the gas-liquid plumes, the bubble velocity and the pierce length were also measured with simultaneous air-blowing from four Tuyeres 1, 2, 4, 5. Figures 11 and 12 show the distribution of the bubble velocity and pierce length at the height range from 30 to 50 mm in Section XZ at $y=35 \text{ mm}$, respectively. Due to the random nature of these measured quantities and the less stability of the measurement caused by gas blowing using the multi-tuyere, the data in figures 11 and 12 look somewhat scattered. It is seen that the x range in the two figures has been cut into two sub-sections, 'a' and 'b'. At sub-section 'a' of figure 11, the bubble velocity values roughly remain uniform. While in sub-section 'b', it decreases with the increasing $|x|$ gradually. It is noticed in figure 12 that either in sub-section 'a' or in 'b', the bubble pierce length variations are not obvious. The average bubble pierce length in sub-section 'b' is somewhat higher than that in sub-section 'a'. The above-mentioned difference in the bubble pierce length may be caused by bubble coalescence resulted from the impingement of the recirculating flow to the upward gas/liquid streams.

(2) In section XOZ.

The results for section XOZ reveal a different situation from those in section XZ at $y=35 \text{ mm}$. Figure 13 shows that the bubble velocity is slightly getting higher at $x=12 \text{ mm}$ and $x=36 \text{ mm}$, i.e. the locations 2 to 4 cm above tuyeres 2 and 4, respectively. More close to the sidewalls, no obvious velocity decrease

has been observed. This may indicate that the effect of the sidewall becomes weaker there at the locations more close to the tuyeres (*i.e.* y is smaller).

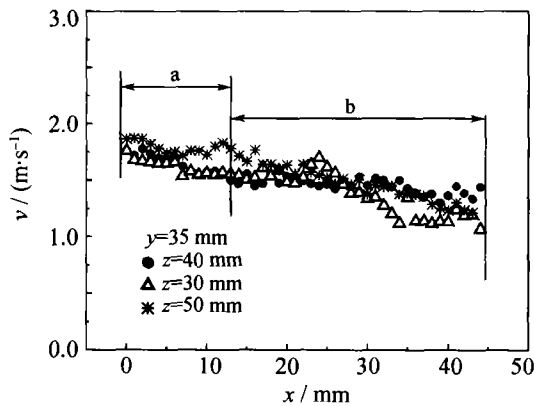


Figure 11 Bubble velocity distribution in Section XZ at $y=35$ mm (using four tuyeres).

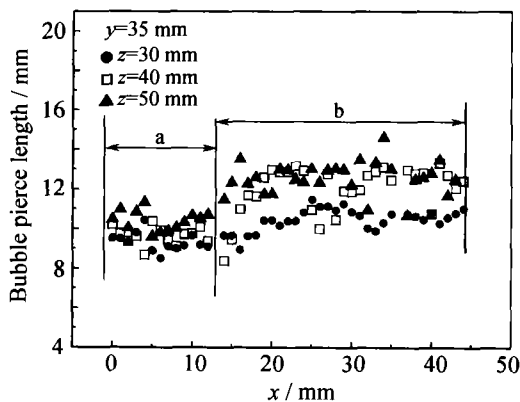


Figure 12 Bubble pierce length distribution in Section XZ at $y=35$ mm (using four tuyeres).

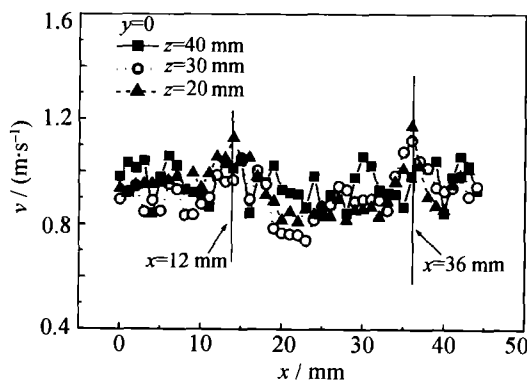


Figure 13 The bubble velocity distribution in Section XOZ (using four tuyeres).

In figure 14 the bubble pierce length distribution in half of the whole section XOZ is illustrated. It can be seen that the bubble pierce length between tuyeres 2 and 4 ($x=0$ to 12 mm in this figure) is roughly uniform. Whereas between tuyeres 4 to 5, the pierce length exhibits only a slow increasing tendency, and the more close to the wall, the more increase can be seen. This may attribute to the coalescence by the impingement of recirculating flow coming from the sidewall to the

up-ward gas stream.

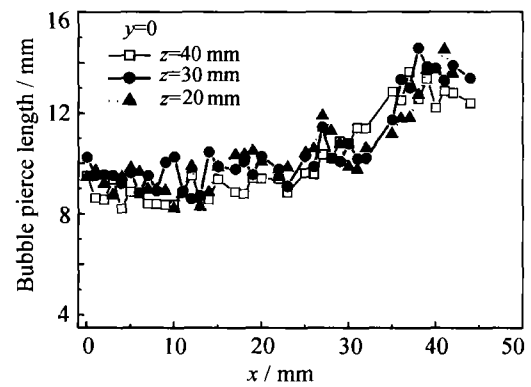


Figure 14 The bubble pierce length distribution in Section XOZ (using four tuyeres).

With a comparison of the geometry between the water model and a real copper, the distribution characteristics for the bubble velocity and the pierce length in sub-section 'a' could be used to characterize those in the region above the tuyeres in a real converter. While the information obtained from sub-section 'b' may indicate the characteristics of those in the regions close to the two vertical walls in the copper converter.

4 Discussion

In the present study, the use of Fr' may imply that the interaction between gas and liquid phase has been the emphasis. A completely physical modeling of bubbles behavior, more dimensionless groups, such as Weber number or Archimedes number, need to be taken into consideration. While the remarkable differences of physical properties, such as the density, viscosity and surface tension between water and copper matte exist, an ideal physical modeling is difficult to be reached. More sophisticated work has to be carried out using a melt with more close physical properties to copper matte. As the initial effort, the present work provides the information regarding major features caused by the interaction between the gas/liquid streams(s) and the molten bath in the copper converter.

It can be noticed that the characteristics of the bubble velocity distribution in this work are similar to those for the void fraction distribution published in a previous report [8]. While different distribution characteristics between the bubble velocity and the pierce length exist. This occurs especially in the regions close to the two vertical sidewalls. The impingement of recirculating flows to the upward gas-liquid streams there may reduce the velocity and the void fraction, however, cause the bubble coalescence.

The chemical reactions, the un-uniform distribution in temperature and pressure in a copper converter may

affect the behavior in the molten bath of a real converter. Nevertheless, the main characteristics obtained from the water model mentioned above would be valid for describing the two-phase zone in a copper converter. The present study together with the information of chemical aspects [8, 10, 11] obtained by present group would be helpful for a better understanding of the kinetic aspect of the operation process in copper converter.

5 Summary and conclusions

The spatial distributions of upward bubble velocity and pierce length in a sectional water model of the copper converter has been measured in the cases of gas injection. Fr' for the model experiments was set equal to that in the converter operation of Guixi Smelter.

In the case of using a single tuyere, the bubble velocity distribution along longitudinal direction is similar with Gaussian function. While beyond the range close to the tuyere centers range, the bubble pierce length exhibits a sudden increase. The bubble velocity at a specified location could vary in a wide range up to a few meters per second. The distribution of its probability obeys a log-normal function. The parameters of the log-normal function vary with the location in the bath. While the bubble pierce length a fixed point varies in a much narrow range below a few centimeters, and the locations corresponding to the peaks of its probability do not exhibit a obvious moving.

In the case of using four tuyeres, the velocity look roughly uniform in the region above the central tuyeres, beyond this region (corresponding to subsection 'b'), the velocity decreased slowly. While bubble pierce length values within both of these two regions look roughly uniform. The average of the bubble pierce length above the central tuyeres is somewhat lower than that in locations beyond the central tuyeres.

The characteristics of the distribution above the central tuyeres may stand for those in region right

above the multiple tuyeres in the copper converter. While those beyond those region may reflect the features of the distributions close to the two ends of the copper converter.

References

- [1] Z.P. Cai and W.S. Wei, Gas liquid hold-up distribution and mathematical modeling of gas-liquid rising velocity in the jet zone of the bottom-blown process [J], *Iron Steel* (in Chinese), 23(1988), No.7, p.19.
- [2] A.H. Castillejos and J.K. Brimacombe, Measurement of physical characteristics of bubbles in gas-liquid plumes: part II Local properties of turbulent air-water plumes in vertically injected jets [J], *Metall. Trans. B*, 18B(1987), p. 649.
- [3] A.H. Castillejos and J.K. Brimacombe, Measurement of physical characteristics of bubbles in gas-liquid plumes: part II Local properties of turbulent air-water plumes in vertically injected jets [J], *Metall. Trans. B*, 18B(1987), p. 659.
- [4] A.H. Castillejos and J.K. Brimacombe, Physical characteristics of gas jets injected vertically upward into liquid metal [J], *Metall. Trans. B*, 20B(1989), p.595.
- [5] Y. Xie, S. Orsten, and F. Oeters, Fluid flow and bubble size distribution in gas-stirred liquid wood's metal, [in] *The Sixth International Iron and Steel Congress* [C], Nagoya, ISIJ, (1990), No.1, p. 421.
- [6] M. Kawakami, N. Tomimoto, and Y. Kitazawa, Estimation of size distribution in iron melt from the chord length distribution [J], *Transactions ISIJ*, 28(1988), p.271.
- [7] G.N. Oryall and J.K. Brimacombe, The physical behavior of a gas jet injected horizontally into liquid metal [J], *Metall. Trans*, 7B(1976), p.391.
- [8] C.L. Chen, J.Y. Zhang, and B. Du, et al., A simulation study on distribution of void fraction in copper converter bath [J], *Trans. Nonferr. Met. Soc. China*, 11(2001), (In press).
- [9] W.S. Wei and Z.P. Cai, The measurement system for study of the characteristics of two-phase flow [J], *Air-dyn. Exp. Meas. Control*, 1992, No.3, p.64.
- [10] C.L. Chen, J.Y. Zhang, S.K. Wei, et al., Thermodynamic study on process in copper converters (The copper-making stage) [J], *J. Univ. Sci. Technol. Beijing*, 7(2000), No.3, p.184.
- [11] C.L. Chen, J.Y. Zhang, M. Bai, et al., Investigation on the copper content of matte smelting slag in Peirce-Smith converter [J], *J. Univ. Sci. Technol. Beijing*, 8(2001), No.3, p.177.